Experimental and Theoretical Dissection of Sodium Cation/Glycine Interactions

R. M. Moision and P. B. Armentrout*

Department of Chemistry, University of Utah, Salt Lake City, Utah 84112

Received: July 17, 2002

The binding of Na^+ to glycine is examined in detail by studying the interaction of the sodium cation with glycine and five molecules that contain the functional components of glycine both singly and in pairs. Bond dissociation energies of Na^+-L where L = glycine, ethanol amine, propionic acid, methyl ethyl ketone, and 1-propylamine are reported, and L = 1-propanol is available in the literature. Experimentally, the bond energies are determined using threshold collision-induced dissociation of the Na^+-L complexes with Xe using a guided ion beam tandem mass spectrometer. Analysis of the energy-dependent cross sections provides 0 K bond energies for the Na^+-L complexes. All bond energy determinations account for unimolecular decay rates, internal energy of reactant ions, and multiple ion−molecule collisions. Ab initio calculations at the MP2-(full)/6-311+G(2d, 2p)//MP2(full)/6-31G* and CBS-QB3 levels, which also include 1-amino-2-propanone, show reasonable agreement with the experimental bond energies and with the few previous experimental values available. The combination of this series of experiments and calculations allows the binding strength of individual functional groups and the influence of chelation to be thoroughly explored. This permits the driving forces for the interaction of Na^+ with glycine to be understood in some detail. Specifically, glycine is a bidentate ligand with Na^+. The primary binding site is the carbonyl with a bond energy reduced by an inductive effect of OH in the carboxylic acid group. Chelation to the amino group enhances the bonding although the increase is mediated by steric constraints imposed by the sp^2 hybridization at the carbon center of the carboxylic acid group.

Introduction

Alkali metal ions interact with a variety of peptides and proteins in biological systems,[1,2] such that there is a fundamental interest in the compilation of preferred binding locations and affinities. Accurate thermodynamic information on the noncovalent interactions in alkali metal systems can play an important role in advancing our understanding of their function in biological systems. Because complications resulting from solvent can be eliminated, measurement of gas-phase affinities is convenient and has the additional advantage of reflecting the intrinsic bond strengths between alkali metal ions and peptides.[3] In addition, peptides charged via complexation with alkali metal ions (e.g., Li^+, Na^+, K^+) have held the promise of greater predictability in localizing the charge, thereby resulting in more selective fragmentation relative to protonation, which would make for more effective mass spectrometric schemes for sequencing information.[3−10] Indeed, alkali cationization has been shown to enhance the CID fragmentation and dissociation of fatty acids,[11] sugars,[8,12] nucleotides,[13] and alcohols.[14]

Thus far, the majority of work on alkali-cationized peptides has concentrated on oligopeptides. One of the primary difficulties in the interpretation of the fragmentation of these larger peptides is that the exact location and coordination of the alkali metal ion is often difficult to determine unequivocally. Even in simple alkali metal ion/amino acid systems, a number of stable, low-energy conformations may exist. For example, glycine, the simplest amino acid, has a number of low-energy conformers resulting from the internal rotational degrees of freedom of the C−N, C−C, and C−O bonds, as well as the possibility of intramolecular hydrogen bonding. In a theoretical study of neutral glycine, Nguyen et al. found seven conformations within 12 kJ/mol of the ground state conformer.[15] The polyfunctionality of glycine further complicates matters because the metal ion can coordinate with several functional groups. Thus, a rigorous understanding of the interaction of even a single amino acid with an alkali metal can present a rather daunting undertaking.

A logical starting point to further our understanding of how alkali metal ions interact with oligopeptides is to begin compiling a quantitative knowledge of how alkali metals interact with a single amino acid. This allows for the building of a "thermodynamic vocabulary" of alkali metal binding so that one can intelligently predict and understand the affinity of a metal ion with more complicated systems. To this end, recent studies in our lab[16−21] and others[22−26] have compiled and reviewed experimental and theoretical values for the binding of sodium cations to a number of small organic molecules.

In the work presented here, we continue to expand our knowledge of sodium affinities by examining in detail the binding of the sodium cation to glycine (GLY). Although this interaction has been studied previously, both experimentally[27,28] and theoretically,[29−33] our approach in this work is to better understand the driving forces behind this complex interaction by dissecting it into smaller parts. To accomplish this, we study the pairwise interactions between the sodium cation and a series of simpler organic molecules that contain the functional "components" of glycine and retain the length of the backbone of the glycine molecule. For instance, methyl ethyl ketone (MEK), 1-propylamine (PAM), and 1-propanol (POH) (previously studied[18,21]) are used to model the binding of sodium to isolated carboxyl, amine, and hydroxyl groups, respectively. Propionic acid (PPA), ethanol amine (EAM), and 1-amino-2-propanone (AMP) were selected to provide models for binding to molecules with pairs of these functional groups. Unfortu-

10.1021/jp0216373 CCC: $22.00
Published on Web 09/28/2002

nately, 1-amino-2-propanone undergoes reductive amination making it unavailable for experimentation, thus, only theoretical calculations were performed for this ligand. This approach allows us to compile the intrinsic binding affinities of individual ligands as well as to begin to quantitatively understand the impact that chelation, electron delocalization, inductive effects, and conformational strain have on the binding strength of bidentate ligands.

In this work, absolute bond dissociation energies (BDEs) of $Na^+(L)$ complexes are measured using threshold collision-induced dissociation (CID) in a guided ion beam tandem mass spectrometer. We provide here the first experimental values for Na^+ binding with ethanol amine, methyl ethyl ketone, propionic acid, and 1-propylamine. Theoretical calculations at the MP2-(full)/6-31G* level are carried out to provide structures, vibrational frequencies, and rotational constants needed for analysis of the threshold CID data. Experimental BDEs are compared to previous experimental values, where available, and to theoretical calculations performed using single point calculations at the MP2(full)/6-311+G(2d,2p) level including zero point energy (ZPE) and basis set superposition error (BSSE) corrections. The inclusion of ZPE effects is particularly important in assessing the relative energies of the complexes considered here. Numerous theoretical studies on the neutral glycine molecule have commented that the inclusion of ZPE is essential to obtain the correct energetic ordering of the neutral conformers.[15,34,35] As an additional check on the accuracy of theory, we have also performed calculations using the CBS-QB3 complete basis set extrapolation protocol.[36]

Experimental and Computational Section

General Experimental Procedures. Cross sections for CID of the metal−ligand complexes are measured using a guided ion beam tandem mass spectrometer (GIBMS) that has been previously described in detail.[37] The metal−ligand complexes are produced as described below. Briefly, metal−ligand complexes are extracted from the source and are mass selected using a magnetic momentum analyzer. The mass selected ions are decelerated to a well-defined kinetic energy and are focused into an rf octopole ion guide that traps the ions radially. This minimizes the loss of the reactant and any product ions resulting from scattering. The octopole passes through a static gas cell containing xenon. Xenon is used as the collision gas for reasons described elsewhere.[38,39] After collision, the parent and product ions drift to the end of the octopole, where they are mass selected using a quadrupole mass filter and are detected with a scintillation ion detector and the signal processed using standard pulse counting techniques.

Ion intensities, measured as a function of collision energy, are converted to absolute cross sections as described previously.[37] Because of the high efficiency of collection in the octopole, relative and absolute cross sections may be determined. The uncertainty in relative cross sections is about ±5%, and the absolute cross section uncertainty is about ±20%. The absolute zero of energy for the ion beam is determined using a retarding potential technique. The result is fit to a Gaussian distribution, which has a fwhm of roughly 0.3 ± 0.1 eV (lab). The uncertainty in the absolute energy scale is ±0.05 eV (lab). Ion kinetic energies in the laboratory frame are converted to energies in the center-of-mass (CM) frame using $E_{cm} = E_{lab}\, m/(m + M)$, where M and m are the masses of the ionic and neutral reactants, respectively. All energies herein are reported in the CM frame unless otherwise noted.

Ion Source. Metalated complexes are generated in a 1 m-long flow tube[40,41] operating at a pressure of 0.5−1.0 Torr with a helium flow rate of 4000−7000 sccm. Sodium ions are generated in a continuous dc discharge by argon ion sputtering of a cathode made from tantalum rod with a small cutout containing sodium metal. Typical operating conditions of the discharge are about 1.7−2.0 kV and 10−20 mA in a flow of approximately 10% argon in helium. The Na^+−L complexes are formed by associative reactions of the sodium ion with the neutral ligands. Neutral ligands are introduced approximately 50 cm downstream from the discharge. Glycine is the only ligand in this study that does not have sufficient volatility to be introduced directly into the flow tube at room temperatures. Glycine is introduced by passing a stream of He over the heated (150−200 °C) solid. The flow conditions described above give approximately 10^4−10^5 collisions between the metal−ligand complex and the buffer gas. This should rotationally and vibrationally thermalize the complexes. All ions produced by this source are therefore assumed to have their internal energy well-described by a Maxwell−Boltzmann distribution of ro-vibrational states at 300 K. Previous work from this laboratory has shown this assumption to be reasonable for a number of systems.[38,40,42−45]

Thermochemical Analysis. The threshold represents the primary bond dissociation energy, assuming that there are no activation barriers present in excess of the endothermicity. Threshold regions of the CID reaction cross sections are modeled using eq 1

$$\sigma(E) = \sigma_0 \sum_i g_i (E + E_i - E_0)^n / E \qquad (1)$$

where σ_0 is an energy-independent scaling factor, n is an adjustable parameter that describes the efficiency of collisional energy transfer,[46] E is the relative kinetic energy of the reactants, and E_0 is the threshold for CID of the ground electronic and ro-vibrational state of the reactant ion. The summation is over the ro-vibrational states of the reactant ions, i, where E_i is the excitation energy of each state and g_i is the population of those states ($\Sigma g_i = 1$). Vibrational frequencies and rotational constants are taken from ab initio calculations, as detailed in the next section. The Beyer−Swinehart algorithm[47−49] is used to evaluate the density of the ro-vibrational states and the relative populations g_i are calculated for a Maxwell−Boltzmann distribution at 300 K. Before comparison with the data, eq 1 is convoluted over the kinetic energy of the reactant and thermal broadening of the neutral gas.[50] Cross sections for a variety of alkali metal ion CID reactions have been reproduced using this model with good accuracy in the resulting thermochemistry.[16,18−21,51−54] In addition, we have recently demonstrated that the cross section form given in eq 1 is consistent with direct measurements of the energy transferred in collisions between $Cr(CO)_6^+$ with Xe,[46] a result that provides increased confidence in the use of this model to obtain accurate thermodynamic information from CID thresholds.

Several systematic issues can obscure the interpretation of the data and must be taken into account during analysis in order to produce accurate thermochemical data. These include the internal energy of reactant ions (which is included explicitly in eq 1), multiple reactant ion/neutral gas collisions, and lifetime effects. To ensure rigorously single collision conditions, data are collected at two or more pressures, generally about 0.2, 0.1, and 0.05 mTorr, and the cross sections are extrapolated to zero pressure prior to analysis. Figure 1 shows an example cross section for the Na^+(EAM) system taken at 0.2 mTorr and the pressure extrapolated (0.0 mTorr) cross section. For the systems studied here, pressure extrapolation generally results in thresh-

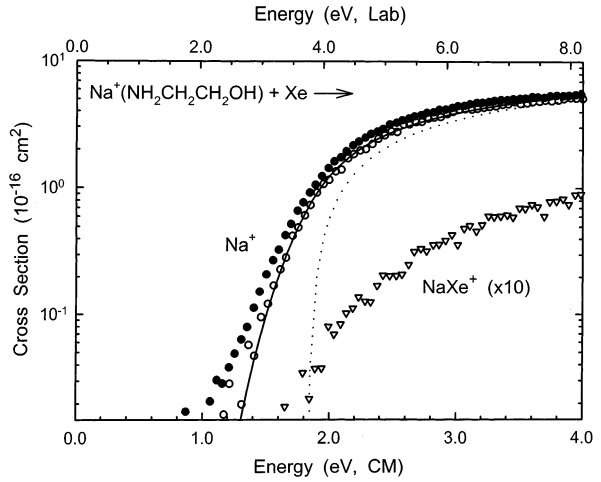

Figure 1. Cross sections for collision-induced dissociation of Na^+-(EAM) with Xe as a function of kinetic energy in the center-of-mass frame (lower *x*-axis) and the laboratory frame (upper *x*-axis). Data are shown for a xenon pressure of 0.2 mTorr (solid circles) and extrapolated to zero (open circles). Cross sections for the ligand exchange process to form $NaXe^+$ are shown by open triangles. The solid line shows the best fit to the extrapolated data using the model in eq 1 convoluted over the internal energy distributions. The dotted line shows the model cross section in the absence of experimental kinetic energy broadening for reactants with an internal energy of 0 K.

olds being 0.02 to 0.03 eV higher than values obtained from data acquired at a collision gas pressure of roughly 0.05 mTorr where only about 4% of the ions undergo a single collision.

As previously discussed,[55] dissociation of large molecules with many internal modes may not occur during the time scale of the experiment, $\sim 10^{-4}$ s. This lifetime effect can produce an observed threshold with an onset delayed from the thermodynamic limit, a kinetic shift, that becomes more noticeable as the size of the molecule increases. These kinetic shifts are estimated by incorporating Rice−Ramsperger−Kassel−Marcus (RRKM) statistical theory,[56] which predicts the unimolecular rate of dissociation of an energized molecule, into eq 1, as described in detail elsewhere.[55] In all of the complexes studied here, we assume that the dissociation occurs with a loose transition state in the phase space limit (PSL) such that the transition states (TSs) are assumed to be product like. Thus, the transitional frequencies, those that become rotations of the completely dissociated products, are treated as rotors. The external rotational constants of the TS are determined by assuming that the TS occurs at the centrifugal barrier for interaction of Na^+ with the neutral ligand, calculated as outlined elsewhere.[55] The 2-D external rotations are treated adiabatically but with centrifugal effects included, consistent with the discussion of Waage and Rabinovitch.[57] In the present work, the adiabatic 2-D rotational energy is treated using a statistical distribution with an average rotational energy, as described in detail elsewhere.[54,55] Analyses with an explicit summation over the possible values of the rotational quantum number were also tested and found to provide nearly identical results. Overall, this PSL model has been shown previously to provide accurate estimation of kinetic shifts for CID processes involving alkali metal ions.[20,51,52,54,55]

Model cross sections calculated using eq 1 are convoluted with the kinetic energy distribution of both reactants and then compared to the reaction cross section using a nonlinear least squares routine and parameters σ_0, n, and E_0 are optimized. These threshold energies are converted to 0 K bond energies by assuming that E_0 represents the energy difference between reactants and products at 0 K. This requires that there are no activation barriers in excess of the endothermicity of dissociation. This assumption has been shown to be generally valid for ion−molecule reactions[58] and for the heterolytic bond cleavage processes under consideration here.[59] Estimates of the uncertainties associated with the measurements of E_0 are obtained from the range of threshold values determined for different data sets, variations associated with uncertainties in the calculated vibrational frequencies (± 10%), and the uncertainty in the absolute energy scale, 0.05 eV (lab). For analyses that include the RRKM lifetime effect, the associated uncertainty is estimated by increasing and decreasing the time assumed to be available for dissociation, 10^{-4} s, by factors of two.

Computational Details. Model structures, vibrational frequencies, and energetics for the neutral ligands and sodiated complexes were obtained using Gaussian 98W.[60] Many of the neutral ligands and sodiated complexes have numerous geometric conformers with energies close to the ground state. In such cases, a number of conformers were tested in calculations to find the global ground state geometry. We assume that the measured threshold energy is from the ground state complex to the ground state of the neutral ligand. Given the length of time available for the complexes to dissociate, we believe this to be a reasonable assumption as the dissociating complex should be able to fully explore phase space, thereby allowing the neutral ligand to reach its low energy conformation upon dissociation.

Geometries for neutral ligands and sodiated complexes were optimized at the MP2(full)/6-31G* level. This level of theory has previously been determined by Hoyau et al.,[23,31,61] as well as our lab,[16,18] to be sufficient for an accurate description of Na^+ complexes. Rotational constants were obtained from the optimized structures and the vibrational frequencies were also calculated at this level. When used in internal energy determinations or for RRKM calculations, the vibrational frequencies were scaled by 0.9646.[62] Vibrational frequencies for the ground-state complexes and ligands are given in Table S1 and rotational constants in Table S2.

Single point energies were calculated at the MP2(full)/6-311+G(2d, 2p) level using the MP2(full)/6-31G* geometries. Zero-point vibrational energy (ZPE) corrections were determined using the scaled vibrational frequencies calculated as described above. Basis set superposition errors (BSSE) were estimated using the full counterpoise method,[63,64] and ranged between 6 and 9 kJ/mol.

To test the accuracy of these calculations, we also carried out complete basis set extrapolations for all complexes at the CBS-QB3 level of theory.[36] This protocol determines geometries and frequencies at the B3LYP/6-311G(2d, d, p) level and includes higher-order correlation corrections at the MP4 and CCSD(T) levels of theory.

Results

Cross Sections for Collision-Induced Dissociation. Experimental cross sections were obtained for the interaction of Xe with $Na^+(L)$ where L = glycine (GLY), 1-propylamine (PAM), methyl ethyl ketone (MEK), propionic acid (PPA), and ethanol amine (EAM). Figure 1 shows representative data for the Na^+-(EAM) system. A complete set of figures for all five systems can be obtained from Figure 1S in the Supporting Information. The most favorable process observed for all complexes is the loss of the intact ligand in the collision-induced dissociation (CID) reaction 2

$$Na^+(L) + Xe \rightarrow Na^+ + L + Xe \qquad (2)$$

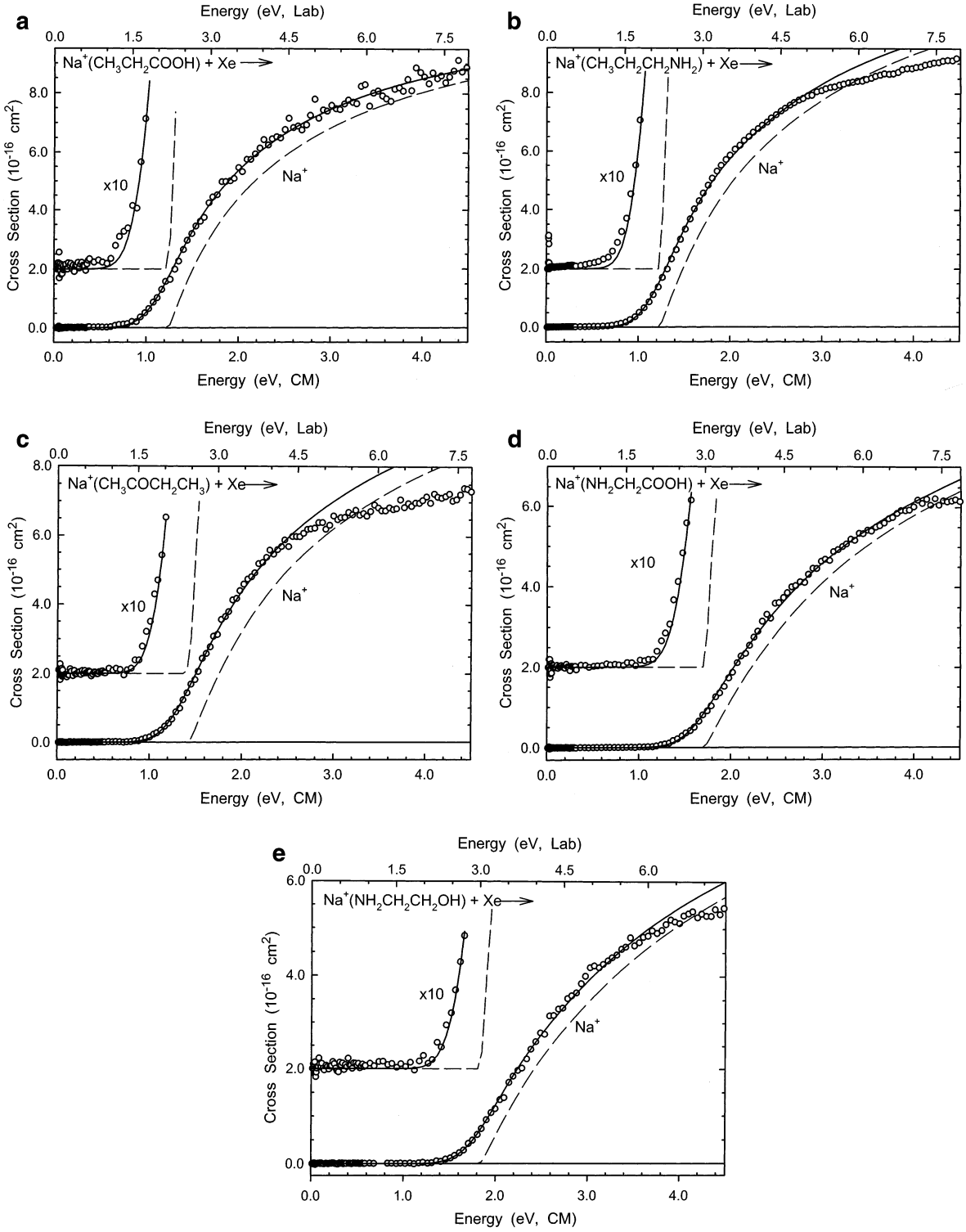

Figure 2. Zero pressure extrapolated cross sections for collision-induced dissociation of $Na^+(L)$ where L = propionic acid, 1-propylamine, methyl ethyl ketone, glycine, and ethanol amine (parts a−e, respectively) with Xe in the threshold region as a function of kinetic energy in the center-of-mass frame (lower *x*-axis) and the laboratory frame (upper *x*-axis). Solid lines show the best fit to the data using the model of eq 1 convoluted over the neutral and ion kinetic and internal energy distributions. Dashed lines show the model cross sections in the absence of experimental kinetic energy broadening for reactions with an internal energy of 0 K.

The only other product observed was a ligand exchange process resulting in the formation of $NaXe^+$, Figure 1. For all of the ligands examined here, the maximum $NaXe^+$ cross section was at least 2 orders of magnitude smaller than for the primary Na^+ product. It is possible that competition between the two channels may cause a shift in the threshold for reaction 2; however, given the intensity of the ligand exchange channel, this shift would be well within our experimental uncertainty.[16,18,54,65] For this and other reasons outlined elsewhere, we have therefore ignored the ligand exchange reaction in our analysis of the CID thresholds.[18]

Threshold Analysis. The model of eq 1 was used to analyze the thresholds for reaction 2 for the five $Na^+(L)$ systems. Figure 2 shows that all experimental cross sections are reproduced by eq 1 over a large range of energies (2−4 eV) and by at least a factor of 100 in magnitude. The results of these analyses are

TABLE 1: Fitting Parameters of eq 1, Threshold Dissociation Energies at 0 K, and Entropies of Activationat 1000 K for CID of Na^+ (L) with Xe[a]

reactant[b]	σ_0	n	E_0 (eV)	E_0(PSL) (eV)	$\Delta S^{\ddagger}_{1000}$ (PSL) (J/Kmol)K^{-1})
Na^+(POH)[c]	16.1 (0.4)	1.1 (0.1)	1.13 (0.04)	1.12 (0.04)	29 (5)
Na^+(PPA)	11.9 (0.6)	1.1 (0.1)	1.24 (0.06)	1.22 (0.06)	21 (5)
Na^+(PAM)	12.7 (0.5)	1.0 (0.1)	1.26 (0.05)	1.25 (0.05)	39 (5)
Na^+(MEK)	11.9 (0.5)	1.1 (0.1)	1.43 (0.06)	1.35 (0.05)	18 (5)
Na^+(GLY)	9.6 (0.5)	1.1 (0.1)	1.74 (0.05)	1.70 (0.05)	40 (5)
Na^+(EAM)	9.0 (0.4)	1.0 (0.1)	1.86 (0.06)	1.81 (0.05)	37 (5)

[a] Uncertainties are listed in parentheses. [b] POH = 1-propanol; PPA = propionic acid; PAM = propylamine; MEK = methyl ethyl ketone; GLY = glycine; EAM = ethanol amine. [c] From Rodgers and Armentrout.[18]

provided in Table 1 along with results for previous work on Na^+(POH).[18,21] Figure 2 shows that there are small "tails" at energies close to the threshold for L = PPA and PAM. The impact of these tails on the threshold values was checked by excluding the tail region during the fit to eq 1. Such analyses showed that the tails led to changes in the threshold energies of less than 0.01 eV in both cases, which is reasonable considering their very small size.

Table 1 includes values for the thresholds, E_0, obtained with and without RRKM lifetime analysis. The size of the kinetic shifts vary from 0.01 eV for Na^+(PAM) to 0.08 eV for Na^+-(MEK). Kinetic shifts vary among the systems because they depend on the dissociation energy (higher E_0 values lead to larger kinetic shifts) and the vibrational frequencies of both the cationized complex and the neutral ligand.

From our analyses, we have also derived values of $\Delta S^{\ddagger}_{1000}$, which give some idea of the looseness of the transition states. These values, listed in Table 1, are in the range determined by Lifshitz[66] for the simple bond cleavage dissociations of several ions. This is reasonable considering that the TS is assumed to lie at the centrifugal barrier for the association of $Na^+ + L$. The rotational contributions to $\Delta S^{\ddagger}_{1000}$ are fairly constant for the complexes studied here. The moderate variations observed in the $\Delta S^{\ddagger}_{1000}$ values are the result of vibrational contributions from the different TS geometries.

Theoretical Results. Structures of the five neutral ligands experimentally studied here along with AMP and POH and for the complexes of these species with Na^+ were calculated as described above. Table 2 gives the bond distances for Na^+ to the oxygen and nitrogen atoms for each of these complexes. Results for the most stable conformation of the sodium ion-ligand complexes are shown in Figure 3. For Na^+(GLY), the present calculations reproduce previous calculations by Hoyau and Ohanessian[31] at the same level of theory. Detailed geometries for neutral ligands and the sodiated complexes are provided in Table S3.

A number of low energy conformations are possible for the sodiated glycine complex. These have been examined in detail by Jensen,[30] Hoyau and Ohanessian,[31] Marino et al.,[32] and to a lesser extent by Wyttenbach et al.[33] and Bouchonnet and Hoppilliard.[29] We performed calculations for the six lowest energy conformations found by Jensen and have decided to use the notation of Jensen to label the sodiated glycine conformers, with the exception that we have termed the zwitterionic structure **ZW** instead of **M2**. We have supplemented this notation with a notation similar to that of Bertrán et al.[67] (in brackets) to describe the sodium binding site of each conformer. For a table comparing the different notations used to describe the glycine conformers in this study and the studies listed above consult Table S4 (in the Supporting Information). Figure 4 shows the relative conformations of these structures. Our MP2 calculations including ZPE corrections indicate that the energy difference between the conformers is only 8 kJ/mol. Calculations by Hoyau and Ohanessian[31] estimate that the barrier required to move between the two lowest energy conformers, from geometry **M1-[CO, N]** to **ZW[COO^-]**, is roughly 70 kJ/mol. The barrier for transformation is well in excess of the thermal energy provided to the complexes in the flow tube. Therefore, it is possible that both of these low energy conformers are present in the flow tube, a possibility that is discussed further below. For the calculated binding energy reported in Table 3, we assume that the glycine complex is in its ground state conformation, **M1-[CO, N]**, prior to CID.

Complexation of Na^+ to these ligands introduces some distortions in the neutral ligand. For the monodentate binding

TABLE 2: MP2(full)/6-31G* Geometry Optimized Structures of the Sodiated Complexes

species[a]	E_{rel} (kJ/mol)[b]	$\Delta_{rel}G_{298}$ (kJ/mol)[c]	Na^+-O bond length (Å)	Na^+-N bond length (Å)	Na^+-C_ωd bond lengths (Å)
Na^+(POH)	0	0	2.202		3.011(β)
	2	1	2.204		3.080(β), 3.125(γ)
Na^+(PAM)	0	0		2.365	3.210(α), 3.532(β), 2.868(γ)
	2	5		2.357	3.178(α), 3.232(β), 4.641(γ)
Na^+(PPA)	0	0	2.313, 2.466 (OH)		2.807(α), 4.304(β), 5.101(γ)
	1	4	2.157, 4.389 (OH)		3.334(α), 4.116(β), 3.724(γ)
Na^+(MEK)	0	0	2.144		3.384(α), 4.375(CH_3), 3.384(β), 4.114(γ)
Na^+(GLY)	0	0	2.261, 4.323 (OH)	2.445	3.029(O), 3.229(N)
M1[N,CO](1)					
ZW[COO^-]	8	9	2.297, 2.346	4.771	2.584(O), 4.122(N)
M3[CO,OH]	9	10	2.320, 2.424 (OH)	4.850	2.729(O), 4.246(N)
M4[N,CO](2)	22	21	2.180, 3.995 (OH)	2.596	2.951(O), 2.896(N)
M5[N,OH]	35	35	4.373, 2.296 (OH)	2.404	3.231(O), 3.208(N)
M8[CO]	52	56	2.154, 4.371 (OH)	5.592	3.360(O), 4.185(N)
Na^+(AMP)	0	0	2.262	2.434	3.224(N), 3.070(O), 4.511(CH_3)
	53	56	2.148	4.140	4.437(N), 3.382(O), 4.269(CH_3)
Na^+(EAM)	0	0	2.251	2.395	3.143(O), 3.104(N)

[a] POH = 1-propanol; PPA = propionic acid; PAM = propylamine; MEK = methyl ethyl ketone; GLY = glycine;AMP = 1-amino-2-propanone; EAM = ethanol amine. [b] Relative energies are calculated at 0 K using MP2(full)/6-311+G(2d,2p) //MP2(full)/6-31G* theory corrected for zero point energies. [c] Relative ΔG_{298} values were calculated using MP2(full)/6-311+G(2d,2p) //MP2(full)/6-31G* theory corrected for zero point energies. Thermal corrections were calculated using standard formulas and molecular constants given in Tables 1S and 2S. [d] For monodentate ligands, ω refers to the carbon atom starting (α) with that nearest to Na^+. For bidentate ligands, ω refers to the carbon atom bound to the amine (N) or carboxyl (O) functional groups. In MEK and AMP, (CH_3) refers to the lone methyl groups.

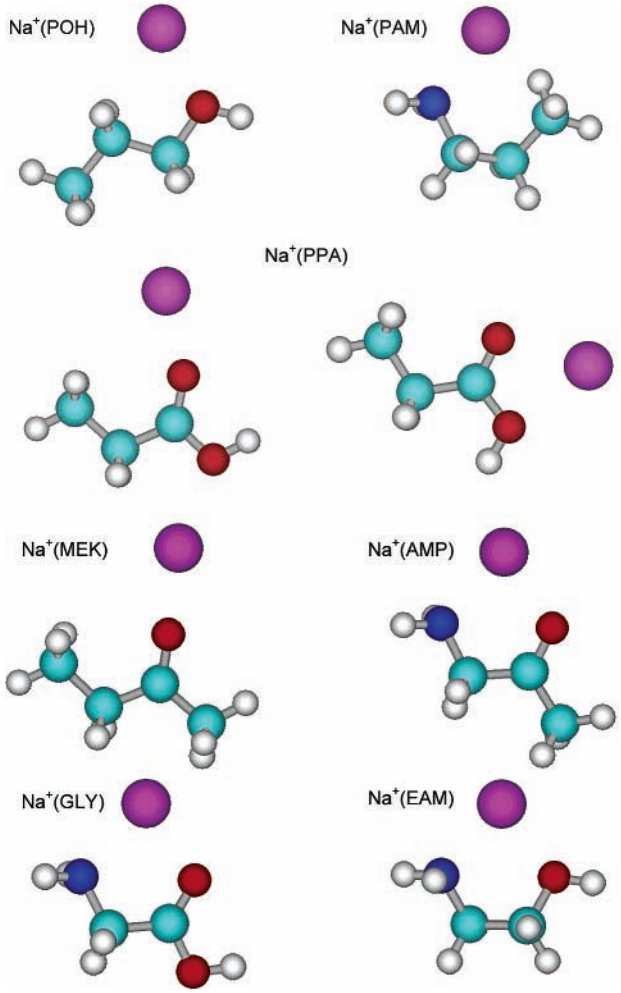

Figure 3. Ground-state geometries of $Na^+(L)$ where L = 1-propanol (POH), 1-propylamine (PAM), propionic acid (PPA) in both the mono and bidentate modes, methyl ethyl ketone (MEK), 1-amino-2-propanone (AMP), glycine (GLY), and ethanol amine (EAM). All structures were optimized at the MP2(full)/6-31G* level of theory.

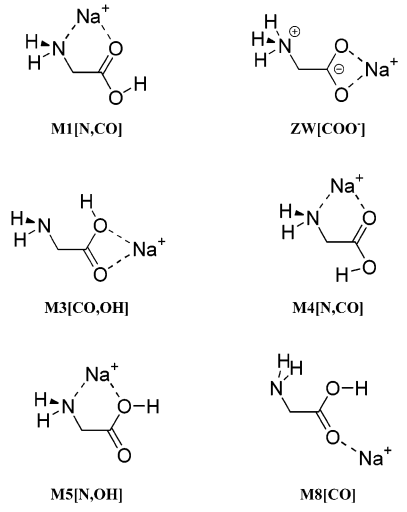

Figure 4. Ground and excited state conformations of Na^+(GLY).

ligands, POH, PAM, and MEK, these distortions are small. For example, in MEK, MP2 calculations show that the association of the Na^+ cation increases the length of the C═O bond from 1.227 to 1.241 Å. The C−C−O bond angles of neutral MEK are fairly symmetric at 121.66° on the methyl side and 121.69° on the ethyl side. In the sodiated complex, the bond angles show slightly more asymmetry and decrease to 120.7° on the methyl side and 121.2° on the ethyl side. In the ground-state Na^+(PAM) conformer, the alkyl tail provides a small amount of stabilization by wrapping around the sodium cation such that the γ-C lies only 2.868 Å away from Na^+ (Table 2). An alternative conformation of the Na^+(PAM) complex lying only 2 kJ/mol higher in energy has the β-C lying only 3.232 Å away from Na^+ and the γ-C much farther away. In the Na^+(POH) system, the analogous structure is the ground state conformer, Figure 3. Here, the relative stabilities are reversed such that the γ-C form, where the γ-C interacts with the Na^+, is 2 kJ/mol less stable than the β-C form. In all of these structures, it is clear that the alkyl group is helping to solvate the alkali metal ion.

PPA can bind either monodentate, where the Na^+ binds solely to the carbonyl oxygen, or bidentate, where the Na^+ is bound to both oxygens in the carboxylic acid moiety. MP2 calculations including ZPE show that the bidentate conformer of PPA is less than 1 kJ/mol lower in energy than the monodentate complex. However, the CBS-QB3 calculations find that the relative energetics of the two complexes reverse with the monodentate complex being 4 kJ/mol lower in energy than the bidentate. This counterintuitive result is because of stabilization afforded from an intramolecular hydrogen bond between the two oxygen atoms, Figure 3. The intramolecular hydrogen bond in the monodentate complex of PPA is significant because it results in a C═O−Na^+ bond angle of 157°, bending the Na^+ away from the hydroxy group, Figure 3. In comparison, the C═O−Na^+ bond angle in the MEK complex is 177° with the Na^+ tilted slightly toward the ethyl side, Figure 3.

There are three bidentate ligands considered in this study: GLY, EAM, and AMP. The low energy conformations of all of these neutral ligands are stabilized by intramolecular hydrogen bonds. This interaction entails the binding of both amine group hydrogens to the carbonyl oxygen in GLY **N1** (Figure 5) and AMP, whereas in EAM, the alcohol group hydrogen binds to the amine nitrogen (similar to GLY **N2**, Figure 5). The primary distortion introduced by the addition of Na^+ involves breaking

TABLE 3: Experimental and Calculated 0 K Enthalpies of Na^+(L) Binding in kJ/mol

complex[a]	expt	CBS-QB3[b]	MP2 (no BSSE)[c]	MP2[d]
Na^+(POH)	113 (4)[e]	108	118	112
Na^+(PPA)	118 (6)	119	119	113
Na^+(PAM)	121 (6)	114	125	118
Na^+(MEK)	131 (7)	132	132	126
Na^+(GLY)	164 (6)	155	161	152
Na^+(AMP)		166	171	162
Na^+(EAM)	175 (7)	165	172	164
MAD[f]		5 (4)	3 (2)	6 (4)

[a] POH = 1-propanol; PPA = propionic acid; PAM = propylamine; MEK = methyl ethyl ketone; GLY = glycine; AMP = 1-amino-2-propanone; EAM = ethanol amine. [b] Calculated using CBS-QB3 complete basis set extrapolation method. [c] Calculated using MP2(full)/6-311+G(2d,2p) //MP2(full)/6-31G* theory corrected for zero point energy. [d] Calculated using MP2(full)/6-311+G(2d,2p)//MP2(full)/6-31G* theory corrected for basis-set superposition error and zero point energy. [e] From Amicangelo and Armentrout.[21] [f] Mean absolute deviation from experimental values.

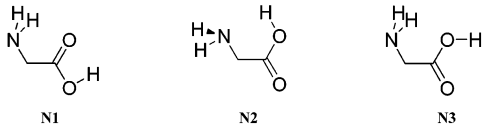

Figure 5. Ground (N1) and low energy conformers (N2 and N3) of neutral glycine from Reference 15.

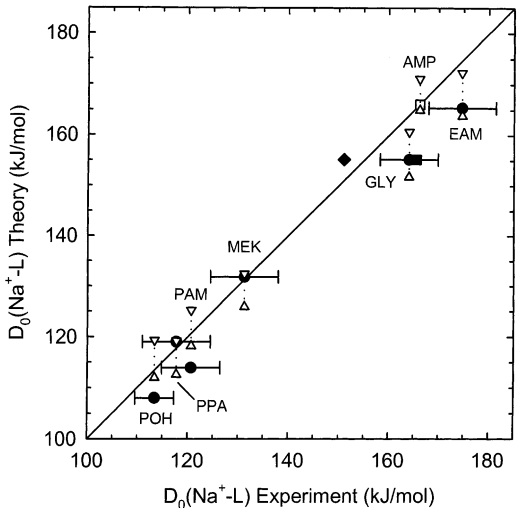

Figure 6. Experimentally measured 0 K bond dissociation energies (in kJ/mol) for $Na^+(L)$ where L = 1-propanol (POH), propionic acid (PPA), 1-propylamine (PAM), methyl ethyl ketone (MEK), glycine (GLY), and ethanol amine (EAM), vs ab initio calculated 0 K bond dissociation energies using the CBS-QB3 protocol (solid circles) and at the MP2(full)/6-311+(2d,2p) //MP2(full)/6-31G* level (in kJ/mol) with BSSE (up triangle) and without BSSE (down triangle). The dotted line connecting the MP2 values is intended as a guide to the reader. Only theoretical values are available for 1-amino-2-propanone (AMP), which is referenced to the CBS-QB3 value (open square). All values are taken from Table 3. Horizontal error bars are for experimental values. The diagonal line indicates the values for which calculated and measured bond dissociation energies are equal. For Na^+(glycine), extra solid symbols indicate experimental values taken from literature and adjusted to 0 K: (diamond, Klassen et al.[27]) and (square, Bojesen et al.[28] as adjusted by Hoyau et al.[31]).

the intramolecular hydrogen bond via rotation of the C−N (in GLY and AMP) or C−O (in EAM) bond to form a pseudo-five-membered ring, e.g. **M1[N, CO]**, Figures 3 and 4. This is driven by Na^+ binding to both the amine nitrogen and the oxygen atom in either a carbonyl (GLY, AMP) or alcohol (EAM) group. The length of the Na^+ bond to oxygen and nitrogen increases in the bidentate ligands relative to the monodentate counterpart, Table 2. For instance, in Na^+(POH), the Na^+-O distance is 2.202 Å, whereas the corresponding Na^+-O bond length in Na^+(EAM) is 2.251 Å. Similar trends are observed for Na^+(PAM) where the Na^+-N bond length is 2.365 Å, whereas the Na^+-N bond lengths are 2.445, 2.434, and 2.395 Å for Na^+(GLY), Na^+(AMP), and Na^+(EAM), respectively. Note that the longer Na^+-N bond lengths in the GLY and AMP complexes indicates that the carbonyl group competes more effectively for the Na^+ than the hydroxy group in EAM, consistent with the relative binding energies of MEK vs POH.

Discussion

Comparison between Theory and Experiment. The sodium cation affinities for the five molecules examined in this study, along with 1-propanol,[18,21] as measured with the guided ion beam mass spectrometer and calculated here are summarized in Table 3. (The experimental value for the Na^+(POH) bond energy used here is taken from Amicangelo et al.[21] who used competitive CID experiments to determine a more precise value but one still consistent with the earlier CID experiments of Rodgers et al.[18]) In all cases, the calculated binding energies refer to the ground state conformations indicated in Table 2. The agreement between theory and experiment is generally very good. The comparison, shown graphically in Figure 6, shows that theory slightly underestimates our experimental values. A comparison of the experimental and theoretically determined values at the MP2 level, including 1-propanol, yields a mean absolute deviation (MAD) of 6 ± 4 kJ/mol, which is comparable to the average experimental uncertainty of about 6 kJ/mol. However, excluding BSSE from the theoretical values gives better agreement with experimental values with a MAD of 3 ± 2 kJ/mol. Feller and co-workers and Ohannesian and co-workers have previously commented that the full counterpoise approximation to BSSE can provide worse agreement with experiment than that of the theoretical values without BSSE corrections in systems such as those studied here.[23,24,68,69] One might expect that the compound CBS-QB3 method would provide better agreement with experiment given that the basis set extrapolation methodologies were developed to provide accurate energetics. Indeed, we find that the CBS-QB3 bond energies give a MAD from experiment of 5 ± 4 kJ/mol.

More detailed comparisons show that the deviations between experiment and theory (for the MP2 calculations including BSSE) are larger for the bidentate ligands, 11 and 12 kJ/mol for EAM and GLY, than for the monodentate ligands, POH, PPA, PAM, and MEK, which have an average deviation of 4 ± 2 kJ/mol. The BSSE corrections for the bidentate ligands are about 1.5 times as large as those of the monodentate ligands, such that excluding these corrections provides a uniformly better prediction of the experimental bond energies. For the four monodentate ligands, MP2 theory without BSSE now overestimates the experimental values by 3 ± 2 kJ/mol. Without BSSE, the theoretical values still underestimate the binding energies of the bidentate ligands, but only by 2−3 kJ/mol. Overall, the utility of BSSE corrections is unclear in these cases. A similar result is observed for the CBS-QB3 values where BDEs to GLY and EAM are low by 9 kJ/mol, and for the 4 monodentate ligands the deviation is an average of 4 ± 3 kJ/mol. Oddly, in contrast to all other ligands, the CBS-QB3 BDEs for Na^+(PAM) and Na^+(POH) are lower than the MP2 (including BSSE) results, and 5−7 kJ/mol lower than experiment, for reasons that are unclear.

As noted above, MP2 theory underestimates the binding energies for the two bidentate ligands experimentally studied here, GLY and EAM, by an average of 12 kJ/mol with BSSE and 3 kJ/mol without BSSE. The only other bidentate ligand involving an amine that we have previously studied is adenine. Here the experimental binding energy of Na^+(adenine) was found to be 140 ± 4 kJ/mol.[70] The theoretical binding energy, calculated at the same MP2 level as used in the present work, was 129 kJ/mol with BSSE and 138 kJ/mol without BSSE. These deviations, 11 and 2 kJ/mol, are almost identical to the ones observed in the GLY and EAM systems. In contrast, comparison of theory (same level) and experiment for a bidentate ligand without nitrogen sites, dimethoxyethane, finds that MP2 theory overestimates the experimental value determined by CID by 9 kJ/mol.[16] Additional experimental and theoretical work on various bidentate systems may be able to further elucidate the origin of these discrepancies between experiment and theory, although the deviations are comparable to the accuracies of either.

The theoretical BDEs reported here are all calculated for the most stable Na^+-L conformation. As noted above, for some of the systems studied here, it is possible that the complexes formed experimentally in the flow tube at thermal energies may consist of multiple low energy conformers. We have provided the relative 0 K energies with ZPE corrections for the complexes that form such low energy conformers in Table 2. In general, if

the barriers between the conformers are substantially larger than kT and if several conformers are readily formed in the flow tube, then experimental formation of several conformations is probable. This would result in the experimental values as determined by CID being low relative to the theoretical determinations, which is counter to the trend observed. In addition, the two low energy conformers of the Na^+(POH), Na^+-(PPA), and Na^+(PAM) complexes differ theoretically by only 2, 1, and 2 kJ/mol, respectively (Table 2). This is the *maximum* error possible if the experimental ions have a population consisting solely of the excited state conformer. Such errors are well within the cited uncertainties. For the complexes with EAM, MEK, and AMP, there is a single conformation considerably lower in energy than the others, such that experimental difficulties associated with alternate conformers are not expected. However, Na^+(GLY) also has a number of low energy conformations, with energy differences small enough to be populated and large enough to affect the experimental threshold. This case is discussed in detail below.

Among experimental problems that could lead to a discrepancy with theory, one possibility is incomplete thermalization of the complex ions. However, this would lead to even higher experimental bond energies, again in disagreement with the relative trends observed here versus theory. Failure to account for multiple collisions would lead to lower experimental bond energies, but neglecting this correction is clearly inappropriate, as demonstrated numerous times previously.[58,71] Another possibility notes that our modeling employs a phase space limit transition state (PSL TS) model, which assumes that the dissociating complex progresses through a "loose" transition state in which the products are only weakly associated as they separate. If the transition states for dissociation were tighter than the PSL TS, then larger kinetic shifts would be observed and this would lower the experimental bond energies. Although this is possible, it was analogous Li^+(alcohol) systems that were used to test whether the use of a PSL TS in modeling CID data adequately reproduces literature thermochemistry.[55] In addition, the PSL TS has been successfully used previously to describe a number of monodentate sodiated complexes,[16,18,19]. Perhaps limitations in the use of the PSL TS are more severe when used to describe bidentate systems such as Na^+(GLY). However, we have previously reported that the PSL TS provides experimental bond energies in good agreement with high-level quantum theory calculations for sodium ions bound in bidentate systems (e.g., dimethoxyethane) as well a variety of crown ether complexes where the sodium is bound tetra-, penta-, and hexadentate.[20,51,52,72]

Conversion to 298 K Values. Because many previous literature values and experimental conditions are tabulated at 298 K, we convert our 0 K bond energies to 298 K bond enthalpies and free energies. The enthalpy conversions are calculated using standard formulas and the vibrational and rotational constants determined at the MP2(full)/6-31G* level of theory. Calculations at the CBS-QB3 level provide comparable values. Table 4 lists 0 and 298 K enthalpy, free energy, and enthalpic and entropic corrections for all systems experimentally determined. Uncertainties in these values are determined by 10% variations in most molecular constants in addition to scaling the metal−ligand frequencies by a factor of 2 in either direction. ΔG_{298} values for all conformers considered in this work were also calculated and relative values are given in Table 2. It can be seen that these values are very similar to those for the 0 K energies.

Comparison to Literature Values. Even though no previous experimental results exist for the binding of Na^+(MEK), the binding of Na^+(acetone) has been examined previously in our lab[16] and others.[23,73] MEK and acetone differ by only a single CH_3 group and so are expected to have similar Na^+ binding energies. The substitution of a CH_3 group for an H will not appreciably change the dipole moment of the ligand, but will increase the polarizability. Work in our laboratory[18] on the binding of short chain alcohols $C_nH_{2n+2}O$ ($n = 1-4$) shows that binding strength increases slightly with greater chain length paralleling the increase in the polarizability of the alcohols. Measurements of Na^+(acetone) using GIBMS yielded a value of 130 ± 4 kJ/mol.[16] Our current GIBMS value for MEK is greater than the GIBMS value for acetone by 1 kJ/mol, Tables 3 and 4, and thus is consistent with the results for acetone. High-pressure mass spectrometry (HPMS) measurements by Hoyau et al. on the Na^+(acetone) system give a value of 128 ± 2 kJ/mol,[23] whereas HPMS measurements by Guo et al. yielded 139 ± 1 kJ/mol.[73] Previous work[16,23] has noted that the sodium affinity values of Castleman are somewhat high, which has recently been shown to be a result of contributions from associative ionization of Na Rydbergs.[74]

Although no previous experimental value exists for the binding of Na^+(PAM), a binding energy of 110 ± 1 kJ/mol was recently reported by Hoyau[23] for methylamine, CH_3NH_2, using HPMS. Again, the greater alkyl chain length will lead to an increase in polarizability of the ligand resulting in a greater binding energy to the Na^+. Alkali binding to both of the analogous alcohol systems, methanol and 1-propanol, have been studied previously in our lab.[18,21,54] The binding of Na^+ to 1-propanol was found to be 16 ± 7 kJ/mol higher than to methanol. Our value of 121 ± 6 kJ/mol for PAM is 10 ± 6 kJ/mol higher than the methylamine value, consistent with the stronger binding observed in the analogous alcohol systems.

There is no other experimental value for the binding affinity of Na^+(PPA). A theoretical ΔH_{298} for Na^+(formic acid) of 99 kJ/mol has been reported by Hoyau et al. calculated at the MP2-(full)/6-311+G(2d,2p)//MP2(full)/6-31G* level.[23] Our ΔH_{298} value of 119 ± 6 kJ/mol for Na^+(PPA), 20 ± 6 kJ/mol higher, is again in agreement with the chain length dependence observed in the alcohol systems. Likewise, there is no other experimental value for the binding affinity of Na^+(EAM). The value of 175 ± 7 kJ/mol is the highest experimental binding energy for the systems studied here.

The only system included in the present work that has been studied extensively is Na^+(GLY). Here, we report an experimental binding energy at 298 K of 166 ± 6 kJ/mol. CID measurements using a triple quadrupole apparatus by Kebarle and co-workers (KABK)[27] yielded a 298 K enthalpy of 153 ± 10 kJ/mol. Measurements by Bojesen et al.[28] using the kinetic method produced a 298 K enthalpy of 159 ± 12−20 kJ/mol.

TABLE 4: Enthalpies and Free Energies of Na^+−L Binding of at 0 and 298 K in kJ/mol[a]

system[b]	ΔH_0c	$\Delta H_{298} - \Delta H_0$d	ΔH_{298}	$T\Delta S_{298}$d	ΔG_{298}
Na^+(POH)	113(4)	1.3(0.2)[e]	114(4)	29(1)	85(4)
Na^+(PPA)	118(6)	0.9(0.1)	119(6)	27(4)	92(6)
Na^+(PAM)	121(6)	3.0(0.2)	124(6)	34(5)	90(6)
Na^+(MEK)	131(7)	0.5(0.1)	132(7)	27(4)	105(7)
Na^+(GLY)	164(6)	2.3(0.2)	166(6)	34(5)	132(6)
Na^+(AMP)[e]	162	2.6	165	38	127
Na^+(EAM)	175(7)	1.9(0.2)	177(7)	32(5)	145(7)

[a] Uncertainties are listed in parentheses. [b] POH = 1-propanol; PPA = propionic acid; PAM = propylamine; MEK = methyl ethyl ketone; GLY = glycine;AMP = 1-amino-2-propanone; EAM = ethanol amine. [c] Experimental values from except for Na^+(AMP), which comes from theory, Table 3. [d] Calculated using standard formulas and molecular constants given in Tables 1S and 2S.

TABLE 5: Experimental and Calculated Na^+(Glycine) 0 K Binding Energies in kJ/mol

experimental method or theoretical level	binding energy[a] no ZPE	binding energy[a] ZPE incl.
MP2/6-31G*//HF/3-21G[b]	189	183[c]
MP2/6-31+G(2d) //HF/6-31G*[c]	161	155[c]
MP2(FC)/6-311+G(2d,2p)//MP2(FC)/6-31G*[i]	**152** (157)	146 (151)
MP2(full)/6-311+G(2d,2p)//MP2(full)/6-31G*[e,i]	**158** (167)	**152** (161)
MP2(FC)/aug-cc-pVTZ//MP2(FC)/aug-cc-pVDZ[h,i]	**154** (155)	**147** (149)
MP2(full)/aug-cc-pVTZ//MP2(full)/aug-cc-pVDZ[h,i]	**157** (165)	**151** (158)
B3P86//6-311+G(2d,2p)//B3P86/6-31G*[i]	**165** (168)	**158** (161)
B3LYP/DZVP//B3LYP/DZVP[f]	180	174[c]
B3LYP/6-311+G(2d,2p)//B3LYP/6-31G*[i]	**169** (172)	**163** (166)
B3LYP/6-311++G**//B3LYP/6-311++G**[g]		164
B3LYP/TZVP//B3LYP/6-311++G**[g]		170
B3LYP/aug-cc-pVTZ//B3LYP/aug-cc-pVDZ[h,i]	**168** (170)	**161** (163)
CCSD/6-31++G**//MP2(full)/aug-cc-pVDZ[h,i]	165	159
QCISD(T,E4T)/6-311G**//MP2(full)/aug-cc-pVDZ[i]	177	170
QCISD(T,E4T)/6-311++G**//MP2(full)/aug-cc-pVDZ[i]	160	153
G2[i]		152
CBS-QB3[i]		155
kinetic method[j]		166
CID triple quadrupole[k]		151 ± 10
CID GIBMS[i]		164 ± 6

[a] Values in bold include BSSE corrections. [b] ref 29. [c] ZPE corrections from geometry and frequency calculations at the MP2(full)/6-31G* level. [d] ref 30. [e] ref 31. [f] ref 33. [g] ref 32. [h] The aug-cc-pVDZ and aug-cc-pVTZ basis sets do not include Na^+. For these calculations, 6-31+G* and 6-311+G*, respectively, were used for Na^+. [i] This work. [j] ref 28, as corrected by Hoyau and Ohanessian, footnote e. [k] ref 27.

This value is only approximate as the authors were unable to find a suitable Na^+ reference base. Instead, it was noted that Na^+ binding energies were close to 75% of the corresponding Li^+ binding energies for a number of compounds studied. The Na^+ scale was therefore anchored by Na^+(alanine), the value of which was set at 75% of the Li^+(alanine) value. The accuracy of this procedure has been criticized and an uncertainty of ± 25 kJ/mol has been estimated.[70] The 159 kJ/mol value for Na^+-(GLY) of Bojesen et al. was recently adjusted by Hoyau and Ohanessian[31] to 168 ± 12−25 kJ/mol, in good agreement with our measurement. This adjustment was performed by resetting the Li^+(alanine) value measured by Bojesen et al. using a newly calculated value for the Li^+(GLY) complex. Because the Na^+-(alanine) value was still determined by taking 75% of the Li^+-(alanine) value, even the revised Na^+(GLY) value remains approximate and its agreement with our value is somewhat fortuitous.

A 298 K binding energy of 162 ± 8 kJ/mol was recently reported for the Na^+(alanine) system by Gapeev and Dunbar using ligand-exchange equilibrium measurements.[75] Because the BDE of Na^+(alanine) should be greater than that of the Na^+-(GLY) (by 6 kJ/mol according to Bojesen et al. [28]), our 166 ± 6 kJ/mol value for Na^+(GLY) could be inconsistent with the Gapeev and Dunbar result. The origin of this discrepancy is unclear, but Gapeev and Dunbar measured free energy differences of alanine vs pyridine binding to Na^+ and then calculated entropic corrections to obtain the enthalpy cited above. It is possible that the treatment of torsional motions, hindered rotors, or other effects could lead to differences in the entropic correction used that would resolve this small discrepancy. In any case, no uncertainty was attributed to the entropic correction, whereas recent estimates in our group suggest that such corrections probably have an uncertainty of 4−8 kJ/mol (one standard deviation). Thus, the final enthalpy value given by Gapeev and Dunbar should probably have a larger uncertainty (9−12 kJ/mol). As noted by these authors, these discrepancies are probably mainly an indication of the uncertainties associated with any experimental measurement of absolute Na^+ affinities.

Table 5 includes a complete list of calculated and experimental BDEs for the Na^+(GLY) system taken from the literature and the present work. To facilitate more uniform comparison, we have added ZPE corrections (with geometries and frequencies calculated at the MP2(full)/6-31G* level) to theoretical values from the literature where this correction was not originally included. For completeness, we have included theoretical values obtained here that use Dunning's correlation-consistent basis sets, aug-cc-pVXZ (X = D and T).[76−78] Stepanian et al. have noted that these basis sets using both the B3LYP and MP2 levels of theory yielded vibrational frequencies in excellent agreement with experiment for neutral glycine.[34] The Na^+(GLY) binding energies (including ZPE corrections) calculated here and in the literature range from 146 to 183 kJ/mol. The 183 kJ/mol value of Bouchonnet and Hoppilliard[29] is the highest value in the table, but was obtained using a small basis set without polarization functions (HF/3-21G) for geometry optimization and MP2/6-31G* for single point energies. Jensen's value of 155 kJ/mol (after our ZPE correction)[30] is 28 kJ/mol lower than that of Bouchonnet and Hoppilliard and was obtained using larger basis sets for single point energies, MP2/6-31+G-(2d), and for geometry optimization, HF/6-31G*. The high value of Bouchonnet and Hoppilliard most likely results from the exclusion of diffuse functions in the single point energy calculation.

In previous work in our lab for a number of Na^+(L) complexes,[16,19] we found that B3LYP methods usually result in sodium ion affinities higher than experimental values (MAD of 8 ± 5 kJ/mol) and other theoretical methods. B3P86, MP2, G2, and CBS-Q calculations in this work gave better agreement with experiment (MADs of 6 ± 3, 5 ± 3, 5 ± 4, and 5 ± 3 kJ/mol, respectively). Comparable results are obtained here with the B3LYP values being higher than other levels of theory. MP2 values obtained with the frozen core (FC) approximation are systematically lower than those obtained with all electrons included in the correlation calculation (full). Use of the correlation consistent basis sets vs comparable standard basis sets provides little change in the bond energies (differences of < 2 kJ/mol). At the QCISD level, inclusion of diffuse functions in the triple-ζ basis set (6-311++G**) results in the binding energy being 17 kJ/mol lower than when the diffuse orbitals are excluded (6-311G**). Thus, reasonable theoretical values

range from 151 to 170 kJ/mol with the highest levels of theory giving 155 (CBS-QB3), 152 (G2), 153 (QCISD), and 159 (CCSD) kJ/mol. A median theoretical value of 159 ± 9 kJ/mol is representative of the range of theoretical values obtained here and in the literature. This is within the uncertainty of any of the three experimental values.

Our results are 13 ± 12 kJ/mol higher than that of KABK.[27] Careful analysis of our data yields no experimental artifacts or alternate data analysis procedures that could yield a CID threshold more consistent with a value as low as 151 kJ/mol. Both experimental bond energies have been determined from CID measurements using the same analysis program to extract the threshold energies, the CRUNCH program developed in our lab.[37,40,55,58] The corrections for kinetic shift (0.04 eV) and for internal energy in both cases are equal simply because identical structures for the starting complex and dissociated ligand were assumed by KABK and in this work. Therefore, the assumptions made during analysis of the threshold cross section cannot be responsible for the discrepancy nor do these assumptions provide any evidence one way or another for the structures probed in either experiment.

There are, however, some subtle yet significant differences in the analysis of the two sets of data for the Na^+(GLY) system. Figure 2d clearly shows that our Na^+(GLY) cross section is reproduced with fidelity throughout the entire threshold region and into the noise of the experiment. In contrast, the cross section of KABK is fit over a smaller energy range, 1.5 to 3.4 eV, compared to our modeling range, 0.6 to 4.0 eV. KABK exclude experimental points very close to the threshold because they found it difficult to model these points, probably because of limitations associated with using a quadrupole in the collision region. The advantages of using an octopole collision cell relative to a quadrupole have been discussed in detail previously.[58,79] Briefly, the potential well in an octopole increases as the inverse sixth power of the radial distance from the octopole axis, whereas the potential well in a quadrupole increases with the inverse square power. This produces a much flatter potential surface in the octopole relative to the quadrupole such that the kinetic energies of ions in an octopole are better defined and less perturbed compared to those in an quadrupole. Further, ion−molecule collisions in the entrance and exit regions of the central quad in a triple quadrupole instrument occur at different applied voltages (those needed for the first and third quads), such that some products are formed under poorly controlled reaction conditions.

The *n* value of KABK from the fit of the cross section to eq 1 is also slightly higher than ours, 1.2 vs 1.1. The higher value of *n* leads to a threshold fit that results in an overall lower threshold energy. Although KABK do take cross sections at two different pressures, 0.1, and 0.2 mTorr, they determined that the cross section was not pressure dependent. Our data, taken at three pressures, ~0.2, 0.1, and 0.05 mTorr, had thresholds determined to be 1.65, 1.67, and 1.69 eV, respectively. The likelihood of secondary collisions in the two instruments should be similar as the collision cell in our GIBMS and the one used by KABK are similar in length, 8.6 and 8.0 cm, respectively. When extrapolated to zero pressure, the threshold is increased by ~0.03 eV compared to the lowest pressure data and 0.06 ± 0.01 eV (6 ± 1 kJ/mol) compared to pressure conditions comparable to KABK. This latter difference can account for some of the 13 ± 12 kJ/mol difference between our value and that of KABK.

Another major difference between the two studies is the source used to generate the complexes. KABK generated complexes using an electrospray ionization source (ESI) in contrast to our dc discharge flow tube source (DC/FT). One intriguing possibility is that the ESI source is producing a significantly different internal energy or conformational distribution of sodiated glycine than the DC/FT source. In the DC/FT source, neutral glycine is introduced into the flow tube by heating it under a stream of He gas. Once it enters the flow tube, the gaseous neutral glycine combines with the Na^+ ions via three-body collisions with the He buffer gas to form the sodiated complex. Because there are a number of low energy Na^+(GLY) conformations, their distribution prior to CID will be largely dependent on two factors: the conformation of neutral glycine present before complexation with the Na^+ and the magnitude of any energetic barriers between conformers of the complexes.

Because of its fundamental role in peptide and protein structure as well as its small size, the conformations of neutral glycine have been the subject of extensive experimental[34,80,81] and theoretical[15,82−85] work. As mentioned above, the potential energy surface of the neutral glycine ligand is quite complicated because of the large amount of conformational mobility from rotation about the three axes defined by the C−O, C−N and C−C bonds. The ground state conformer has been theoretically determined and experimentally verified to be the **N1** conformer, Figure 5. It is estimated that in the gas phase at 500 K, the **N1** conformer is approximately 70% of the conformational population.[15,34,80] As mentioned previously, the **N1** form is similar to the conformation that glycine adopts in the low energy **M1-[N,CO]** complex with the amine and carbonyl groups in a syn arrangement, Figure 4; however, the neutral **N1** form has the NH_2 hydrogen-bound to the carbonyl. Experimental and theoretical studies generally agree that a mixture of the **N2** and **N3** conformations of glycine, with the amine and carbonyl groups in an anti arrangement, make up the majority of the remaining gas phase conformational distribution.[15,80,81,83] As noted above, theoretical calculations on the relative energies of the glycine conformers are quite sensitive to the vibrational frequencies. Consequently, there is substantial debate over the relative amounts of **N2** and **N3** present in the gas phase. Nevertheless, at 300 K, the temperature in the DC/FT, we would expect roughly 85% of the neutral population to be the **N1** conformer with the remaining 15% of the population consisting of primarily the **N2** and **N3** conformations.

Because it is likely that the DC/FT will have both the **N1** and **N2** forms of neutral glycine present, introduction of Na^+ should form the **M1[N,CO]** ground state conformer in abundance, and conceivably the **M3[CO,OH]** excited conformation of sodiated glycine. Other conformations are too high in energy (Table 2) to be plausibly formed and the experimental data are inconsistent with the presence of such high energy conformers. Calculations indicate that the **M3[CO,OH]** conformation can undergo a barrierless proton transfer from the hydroxy group to the amino group to form the **ZW[COO^-]** conformer, which is ~1 kJ/mol lower in energy than **M3[CO,OH]**, Table 2.[31] Because the **N1** conformer is dominant in the gas phase and the **M1[N,CO]** is the low energy sodiated complex, one would expect the DC/FT to produce the **M1[N,CO]** complex with >85% probability and it is possible that some complexes could have the **ZW[COO^-]** conformation. To estimate the effect that having a small population of the excited state conformation in our ion beam, we simulated a cross section with a conformer population of 0.85:0.15 **M1[N,CO]**:**M3[CO,OH]**. Threshold analysis of this simulated cross section gives a threshold energy lower by ~2 kJ/mol relative to analysis of a cross section

corresponding to a population consisting entirely of the **M1-[N,CO]** conformer. Thus, we expect that our measurement of the **M1[N,CO]** BDE is accurate within the stated experimental uncertainties. If excited conformations are present, then our experimental value is too low, increasing the discrepancy with theory.

In the ESI source, the sodiated glycine complexes are preformed in solution. The isoelectric point (p*I*) of glycine is 5.97, and therefore in aqueous solution, glycine will be primarily in its zwitterionic form from roughly pH 4−8. Therefore, in solution, complexation with Na^+ is likely to form the zwitterionic **ZW[COO$^-$]** conformer. Although the neutral glycine ligand has not been observed in the zwitterionic form in the gas phase, the zwitterion is greatly stabilized through the interaction with the metal ion. In the gas phase, theoretical calculations show that the sodiated zwitterionic form is only ∼8 kJ/mol higher in energy than the ground-state complex, Table 2. Therefore, volatilization of the **ZW[COO$^-$]** complex directly into the gas phase via ESI seems plausible. Hoyau and Ohanessian[31] recently investigated the interconversion of the Na^+(GLY) isomers in detail and estimated the barrier for transformation from the zwitterion **ZW[COO$^-$]** to the low energy **M1[N, CO]** structure to be approximately 70 kJ/mol. Such a barrier would make it difficult for the two forms to interconvert at the thermal energies available in the ESI source, such that both forms are probably stable in the gas phase. Consequently, it is possible that Na^+(GLY) complexes formed by ESI are largely in their zwitterionic form. However, in the gas-phase, the **ZW[COO$^-$]** conformer can readily rearrange to the **M3[CO,OH]** conformation, such that these would be in equilibrium in the flow tube. Energy differences between these forms depend on the level of theory with the zwitterion conformer more stable than **M3[CO,OH]** by 1 kJ/mol for our MP2 calculations including ZPE corrections (which change this relative value by over 4 kJ/mol), whereas B3LYP calculations of Marino et al.[32] find that **M3[CO,OH]** is more stable by 10 kJ/mol at 298 K. Thus, depending on the relative populations of the three conformers, the resulting experimental threshold could be between 7 and 17 kJ/mol lower than that of the **M1-[N,CO]** conformation. The difference between our binding energy reported here and that of KABK (∼13 kJ/mol) is consistent with the possibility that the ESI is producing a population with a high percentage of the **ZW[COO$^-$]** and **M3-[CO,OH]** species whereas the DC/FT source is producing primarily the **M1[N,CO]** conformer.

Qualitative Trends. The ligands examined in this study can be broken into two categories, ligands with a single binding site (POH, PAM, MEK, PPA) and ones that can bind bidentate (EAM, GLY, AMP). Previous work in this lab has shown that there are a number of factors that can influence the strength of Na^+ binding.[16,18−20] These include the nature of the donor atom, the localization of the electron density on the donor (orbital overlap with the metal ion), electrostatic interactions (polarizability, charge-dipole, and charge-quadrupole), and the possibility of multiple donor (chelation) interactions. For a hard ion such as Na^+, one expects the binding to be primarily electrostatic. This is especially evident in the monovalent binding ligands (POH, PAM, MEK) where the Na^+ binds along the dipole moment of the ligand. For these ligands with a single functional group, the relative binding strength is found to be $=O > NH_2 > OH$, Table 3. We have noted before that species such as NH_3 and CH_3NH_2 bind to Na^+ more strongly than the analogous H_2O and CH_3OH ligands.[16]

Although binding to a carbonyl group is favorable, when this functionality is part of a carboxylic acid group, the binding energy is reduced. Comparison of the Na^+(PPA) complex with Na^+(MEK) shows that the former complex is more weakly bound than the latter complex by 13 kJ/mol. The C−O−Na^+ bond angles, 157° in Na^+(PPA) and 177° in Na^+(MEK), also reflect the different nature of the carbonyl-Na^+ binding in these complexes. The weaker binding of the Na^+(PPA) provides evidence that electron withdrawing effects of the OH group in the carboxylic acid reduce the binding to Na^+.

The situation is much more interesting with the bidentate ligands because the Na^+ has to share the electron density of two binding groups, but the steric limitations of the ligand prevent the Na^+ from optimally aligning with the dipole of either group. This results in an energetic tradeoff where the ligand reorients in order to maximize the Na^+ binding strength, while simultaneously trying to minimize steric strain. Ultimately, the strength of Na^+ binding in bidentate ligands will depend not only on the intrinsic binding affinity of the functional groups involved but on also how much conformational mobility the ligand has to facilitate efficient binding of each group.

Misalignment with the carbonyl dipole affects the binding energy in the GLY and AMP complexes. Using theoretical calculations, we can estimate how much the binding is affected when the Na^+ is located in a nonideal position. We started with the optimized Na^+(MEK) complex and adjusted the bond length and angle of the C=O−Na^+ bond in MEK to that of GLY (2.261 Å, 117.3°). Calculations at the MP2(full)/6-311+(2d,2p) level of this "mutated" Na^+(MEK) structure yielded an energy ∼55 kJ/mol higher than the ground state. In Na^+(GLY), this energy loss is compensated by chelation with the amino group, leading to an overall stronger bond. Identical calculations on a mutated Na^+(PPA) complex result in an energy ∼23 kJ/mol higher than the ground state. The large (32 kJ/mol) difference in the binding energies of the mutated MEK and PPA complexes is partly the result of the ground state of Na^+(PPA) having its C=O−Na^+ bond already tilted at angle of 157°.

All of the bidentate ligands in this study, AMP, GLY, and EAM, contain an amine group and so the second functional group present will have a major impact on the overall binding strength of the Na^+. For AMP, GLY, and EAM, this second group is a carbonyl (as in MEK), carboxylic acid (as in PPA), and alcohol (as in POH), respectively. Given that Na^+ binds more strongly to MEK than POH by 18 kJ/mol, one might predict that AMP would possess a greater binding affinity than EAM. In fact, theory predicts that Na^+ binds EAM and AMP with similar bond energies (within 2 kJ/mol), Table 3.

This energetic tradeoff may be further understood by examining the pseudo five-membered rings formed when Na^+ binds to these ligands, Figure 3. The rings formed by Na^+ with AMP and GLY are very similar in geometry because the planar sp^2 carbon centers in these ligands restrict the distortions the ring can undergo to relieve torsional strain. The dihedral angle of the N−C−C−O portion of the ring is 14° for Na^+(AMP) and 16° for Na^+(GLY). This slight distortion from a planar structure allows the C−N bond to rotate ∼35° in both the GLY and AMP complexes so that the amine hydrogens are only partially eclipsed with the hydrogens on the adjoining carbon atom (0° = fully eclipsed, 60° = fully staggered). In comparison, the carbon in EAM has sp^3 hybridization, which results in a N−C−C−O dihedral angle of 58° in the Na^+(EAM) complex. Here the C−N bond can rotate ∼53° yielding an almost fully staggered configuration of the amine hydrogens. The sp^3 hybridized carbon center in EAM allows the ligand to have a greater amount of rotational mobility relative to AMP and GLY, where the carbon is sp^2 hybridized. This allows the EAM to

better align both the OH and NH_2 dipoles to Na^+ while encountering minimum steric strain. The consequence of AMP and GLY having more rigid sp^2 carbon centers is that these ligands are simply unable to align their carbonyl and amine dipoles to the Na^+ without encountering some steric strain.

Conclusion

The kinetic energy dependence of the collision-induced dissociation of $Na^+(L)$, L = glycine, ethanol amine, propionic acid, methyl ethyl ketone, and 1-propylamine, with Xe are examined in a guided ion beam mass spectrometer. The dominant dissociation process in all cases is formation of $Na^+ + L$. Thresholds at 0 K for these processes are determined after consideration of the effects of reactant internal energy, multiple collisions with Xe, and lifetime effects using a phase space limit transition state model. The experimental results for $Na^+(L)$ are generally in good agreement with ab initio calculations using the CBS-QB3 basis set extrapolation protocol as well as the MP2(full)/6-311+(2d,2p)//MP2(full)/6-31G* level of theory, especially if basis set superposition errors are not included.

Values reported here for ethanol amine, propionic acid, methyl ethyl ketone, and 1-propylamine constitute the first experimental determinations of the sodium cation binding affinities. The value reported here for glycine is higher than a result previously reported by Kebarle and co-workers.[27] Several explanations for the discrepancy are discussed including the possibility that different conformers are being probed. Theoretical results also indicate that several low-energy conformers exist for a number of the complexes studied here. Such conformers could complicate the experimental results, but are unlikely to change the absolute values outside the experimental uncertainties. Theoretical calculations for the complexes of the bidentate glycine and ethanol amine ligands underestimate the experimentally determined binding energies, possibly a result of overestimation of the basis set superposition error.

The experimental results obtained here permit a systematic evaluation of the binding of Na^+ to glycine, thereby allowing a dissection of the interactions involved. From the monodentate ligands, it is clear that the best binding site in glycine is the carbonyl group; however, because this is tied up in a carboxylic acid group, the binding energy is reduced. Enhancement of the binding can be provided by chelation and this occurs to the amine group, the next most strongly binding functional group after the carbonyl. Chelation increases the binding energy but is not additive because of the geometric constraints imposed by binding to both groups. Hence, the charge solvated structure, **M1[N,CO]**, found theoretically to be the ground-state structure for $Na^+(GLY)$ can be easily rationalized as the most stable structure given the individual metal−ligand bond energies determined here. However, quantitative assessment of the bond energy to glycine cannot be accomplished by simply adding up contributions from individual functional groups, a consequence of geometric constraints, as noted previously for systems such as the crown ethers.[20,72] Such effects should be quantifiable to at least first order, holding the promise that accurate estimates of metal ion bond energies to even very complicated systems of biological relevance can be elucidated by a thorough understanding of the individual interactions.

Acknowledgment. Funding for this work was provided by the National Science Foundation under Grant No. CHE-0135517. R.M.M. wishes to thank C. Tracewell for providing valuable experimental advice.

Supporting Information Available: Table S1 lists vibrational frequencies and average vibrational energies at 298 K of the neutral molecules and sodiated complexes determined from vibrational analysis at the MP2(full)/6-31G* level. Table S2 lists rotational constants for the sodiated complexes and products for all five $Na^+(L)$ systems calculated at the same level of theory. Table S3 contains Cartesian coordinates for the neutral ligands and sodiated complexes calculated at the MP2(full)/6-31G* level. Table S4 compares the nomenclature of Na^+-(glycine) complexes from this work and others. This material is available free of charge via the Internet at http://pubs.acs.org.

References and Notes

(1) da Silva, J. J. R. F.; Williams, R. J. P. *The Biological Chemistry of the Elements: The Inorganic Chemistry of Life*; Oxford University Press: New York, 1991.
(2) Wilkins, P. C.; Wilkins, R. G. *Inorganic Chemistry in Biology;* Oxford University Press: New York, 1997.
(3) Teesch, L. M.; Orlando, R. C.; Adams, J. *J. Am. Chem. Soc.* **1991**, *113*, 3668.
(4) Lin, T.; Glish, G. L. *Anal. Chem.* **1998**, *70*, 5162.
(5) Lee, S.-W.; Kim, H. S.; Beauchamp, J. L. *J. Am. Chem. Soc.* **1998**, *120*, 3188.
(6) Mallis, L. M.; Russell, D. H. *Anal. Chem.* **1986**, *58*, 1076.
(7) Renner, D.; Spiteller, G. *Biomed. Environ. Mass Spectrom.* **1988**, *15*, 75.
(8) Cerny, R. L.; Tomer, K. B.; Gross, M. L. *Org. Mass Spectrom.* **1986**, *21*, 655.
(9) Grese, R. P.; Gross, M. L. *J. Am. Chem. Soc.* **1990**, *112*, 5098.
(10) Teesch, L. M.; Adams, J. *J. Am. Chem. Soc.* **1991**, *113*, 812.
(11) Adams, J.; Gross, M. L. *Anal. Chem.* **1987**, *59*, 1576.
(12) Röllgen, F. W.; Giessmann, U.; Borchers, F.; Levsen, K. *Org. Mass Spectrom.* **1978**, *13*, 459.
(13) Mallis, L. M.; Raushel, F. M.; Russell, D. H. *Anal. Chem.* **1987**, *59*, 980.
(14) Adams, J.; Gross, M. L. *J. Am. Chem. Soc.* **1986**, *108*, 6915.
(15) Nguyen, D. T.; Scheiner, A. C.; Andzelm, J. W.; Sirois, S.; Salahub, D. R.; Hagler, A. T. *J. Comput. Che.* **1997**, *18*, 1609.
(16) Rodgers, M. T.; Armentrout, P. B. *J. Phys. Chem. A* **2000**, *104*, 2238.
(17) Rodgers, M. T.; Armentrout, P. B. *Mass Spectrom. Rev.* **2000**, *19*, 215.
(18) Rodgers, M. T.; Armentrout, P. B. *J. Phys. Chem. A* **1999**, *103*, 4955.
(19) Amicangelo, J. C.; Armentrout, P. B. *J. Phys. Chem. A* **2000**, *104*, 11420.
(20) More, M. B.; Ray, D.; Armentrout, P. B. *J. Am. Chem. Soc.* **1999**, *121*, 417.
(21) Amicangelo, J. C.; Armentrout, P. B. Work in progress.
(22) Fujii, T. *Mass Spectrom. Rev.* **2000**, *19*, 111.
(23) Hoyau, S.; Norrman, K.; McMahon, T. B.; Ohanessian, G. *J. Am. Chem. Soc.* **1999**, *121*, 8864.
(24) McMahon, T. B.; Ohanessian, G. *Chem. Eur. J.* **2000**, *6*, 2931.
(25) Rodgers, M. T. *J. Phys. Chem. A* **2001**, *105*, 2374.
(26) Rodgers, M. T. *J. Phys. Chem. A* **2001**, *105*, 8145.
(27) Klassen, J. S.; Anderson, S. G.; Blades, A. T.; Kebarle, P. *J. Phys. Chem.* **1996**, *100*, 14 218.
(28) Bojesen, G.; Breindahl, T.; Andersen, U. N. *Org. Mass Spectrom.* **1993**, *28*, 1448.
(29) Bouchonnet, S.; Hoppilliard, Y. *Org. Mass Spectrom.* **1992**, *27*, 71.
(30) Jensen, F. *J. Am. Chem. Soc.* **1992**, *114*, 9533.
(31) Hoyau, S.; Ohanessian, G. *Chem. Eur. J.* **1998**, *4*, 1561.
(32) Marino, T.; Russo, N.; Toscano, M. *J. Inorg. Biochem.* **2000**, *79*, 179.
(33) Wyttenbach, T.; Witt, M.; Bowers, M. T. *J. Am. Chem. Soc.* **2000**, *122*, 3458.
(34) Stepanian, S. G.; Reva, I. D.; Radchenko, E. D.; Rosado, M. T. S.; Duarte, M. L. T. S.; Fausto, R.; Adamowicz, L. *J. Phys. Chem. A* **1998**, *102*, 1041.
(35) Bludský, O.; Chocholoušová, J.; Jaroslav, V.; Huisken, F.; Hobza, P. *J. Chem. Phys.* **2000**, *113*, 4629.
(36) Montgomery, J. A., Jr.; Frisch, M. J.; Ochterski, J. W.; Petersson, G. A. *J. Chem. Phys.* **1999**, *110*, 2822.
(37) Ervin, K. M.; Armentrout, P. B. *J. Chem. Phys.* **1984**, *83*, 166.
(38) Dalleska, N. F.; Honma, K.; Armentrout, P. B. *J. Am. Chem. Soc.* **1993**, *115*, 12 125.
(39) Aristov, N.; Armentrout, P. B. *J. Phys. Chem.* **1986**, *90*, 5135.
(40) Schultz, R. H.; Crellin, K. C.; Armentrout, P. B. *J. Am. Chem. Soc.* **1992**, *113*, 8590.
(41) Schultz, R. H.; Armentrout, P. B. *Int. J. Mass Spectrom. Ion Processes* **1991**, *107*, 29.

(42) Dalleska, N. F.; Tjelta, B. L.; Armentrout, P. B. *J. Phys. Chem.* **1994**, *98*, 4191.
(43) Fisher, E. R.; Kickel, B. L.; Armentrout, P. B. *J. Phys. Chem.* **1993**, *97*, 10 204.
(44) Khan, F. A.; Clemmer, D. E.; Schultz, R. H.; Armentrout, P. B. *J. Phys. Chem.* **1993**, *97*, 7978.
(45) Schultz, R. H.; Armentrout, P. B. *J. Chem. Phys.* **1992**, *96*, 1046.
(46) Muntean, F.; Armentrout, P. B. *J. Chem. Phys.* **2001**, *115*, 1213.
(47) Beyer, T. S.; Swinehart, D. F. *Comm. Assoc. Comput. Machines* **1973**, *16*, 379.
(48) Stein, S. E.; Rabinovich, B. S. *Chem. Phys. Lett.* **1977**, *49*, 1883.
(49) Stein, S. E.; Rabinovich, B. S. *J. Chem. Phys.* **1973**, *58*, 2438.
(50) Chantry, P. J. *J. Chem. Phys.* **1971**, *55*, 2746.
(51) More, M. B.; Ray, D.; Armentrout, P. B. *J. Phys. Chem. A* **1997**, *101*, 7007.
(52) More, M. B.; Glendening, E. D.; Ray, D.; Feller, D.; Armentrout, P. B. *J. Phys. Chem.* **1996**, *100*, 1605.
(53) Ray, D.; Feller, D.; More, M. B.; Glendening, E. D.; Armentrout, P. B. *J. Phys. Chem.* **1996**, *100*, 16116.
(54) Rodgers, M. T.; Armentrout, P. B. *J. Phys. Chem. A* **1997**, *101*, 2614.
(55) Rodgers, M. T.; Ervin, K. M.; Armentrout, P. B. *J. Chem. Phys.* **1997**, *106*, 4499.
(56) Gilbert, R. G.; Smith, S. C., *Theory of Unimolecular and Recombination Reactions*; Blackwell Scientific: London, 1990.
(57) Waage, E. V.; Rabinovitch, B. S. *Chem. Rev.* **1970**, *70*, 377.
(58) Armentrout, P. B. In *Advances in Gas-Phase Ion Chemistry*; Adams, N. G., Babcock, L. M., Eds.; JAI Press Inc.: Greenwich, CT, 1992; Vol. 1; p 83.
(59) Armentrout, P. B.; Simons, J. *J. Am. Chem. Soc.* **1992**, *114*, 8627.
(60) Frisch, M. J.; Trucks, G. W.; Schlegel, H. B.; Scuseria, G. E.; Robb, M. A.; Cheeseman, J. R.; Zakrzewski, V. G.; Montgomery, J. A., Jr.; Stratmann, R. E.; Burant, J. C.; Dapprich, S.; Millam, J. M.; Daniels, A. D.; Kundin, K. N.; Strain, M. C.; Farkas, O.; Tomasi, J.; Barone, V.; Cossi, M.; Cammi, R.; Mennucci, B.; Pomelli, C.; Adamo, C.; Clifford, S.; Ochterski, J.; Petersson, G. A.; Ayala, P. Y.; Cui, Q.; Morokuma, K.; Malick, D. K.; Rabuck, A. D.; Raghavachari, K.; Foresman, J. B.; Cioslowski, J.; Ortiz, J. V.; Stefanov, B. B.; Liu, G.; Liashenko, A.; Piskorz, P.; Komaromi, I.; Gomperts, R.; Martin, R. L.; Fox, D. J.; Keith, T.; Al-Laham, M. A.; Peng, C. Y.; Nanayakkara, A.; Gonzalez, C.; Challacombe, M.; Gill, P. M. W.; Johnson, B.; Chen, W.; Wong, M. W.; Andres, J. L.; Gonzalez, C.; Head-Gordon, M.; Replogle, E. S.; Pople, J. A. *Gaussian 98*, revision A.7; Gaussian, Inc.: Pittsburgh, PA, 1998.
(61) Hoyau, S.; Ohanessian, G. *Chem. Phys. Lett.* **1997**, *280*, 266.
(62) Foresman, J. B.; Frisch, A. E., *Exploring Chemistry with Electronic Structure Methods;* 2nd ed.; Gaussian, Inc.: Pittsburgh, PA, 1996.
(63) Boys, S. F.; Bernardi, R. *Mol. Phys.* **1970**, *19*, 553.
(64) van Duijneveldt, F. B.; van Duijneveldt de Rijdt, J. G. C. M.; van Lenthe, J. H. *Chem. Rev.* **1994**, *94*, 1873.
(65) Rodgers, M. T.; Armentrout, P. B. *J. Chem. Phys.* **1998**, *109*, 1787.
(66) Lifshitz, C. *Adv. Mass Spectrom.* **1989**, *11*, 713.
(67) Bertran, J.; Rodriguez-Santiago, L.; Sodupe, M. *J. Phys. Chem. B.* **1999**, *103*, 2310.
(68) Feller, D.; Glendening, E. D.; Woon, M. W.; Feyereisen, J. *J. Chem. Phys.* **1995**, *103*, 3526.
(69) Feller, D. *Chem. Phys. Lett.* **2000**, *322*, 543.
(70) Rodgers, M. T.; Armentrout, P. B. *J. Am. Chem. Soc.* **2000**, *122*, 8548.
(71) Armentrout, P. B. *J. Am. Soc. Mass Spectrom.* **2002**, *13*, 419.
(72) Armentrout, P. B. *Int. J. Mass Spectrom.* **1999**, *193*, 227.
(73) Guo, B. C.; Conklin, B. J.; Castleman, A. W. *J. Am. Chem. Soc.* **1989**, *111*, 6506.
(74) Gilligan, J. J.; McCunn, L. R.; Leskiw, B. D.; Herman, Z.; Castleman, A. W. *Int. J. Mass Spectrom.* **2001**, *204*, 247.
(75) Gapeev, A.; Dunbar, R. C. *J. Am. Chem. Soc.* **2001**, *123*, 8360.
(76) Dunning, T. H. *J. Chem. Phys.* **1989**, *90*, 1007.
(77) Kendall, R. A.; Dunning, T. H.; Harrison, R. J. *J. Chem. Phys.* **1992**, *96*, 6796.
(78) Woon, D. E.; Dunning, T. H. *J. Chem. Phys.* **1993**, *98*, 1358.
(79) Armentrout, P. B. *Int. J. Mass Spectrom.* **2000**, *200*, 219.
(80) Iijima, K.; Tanaka, K.; Onuma, S. *J. Mol. Struct.* **1991**, *246*, 257.
(81) Suenram, R. D.; Lovas, F. J. *J. Am. Chem. Soc.* **1980**, *102*, 7180.
(82) Kaschner, R.; Hohl, D. *J. Phys. Chem. A* **1998**, *102*, 5111.
(83) Császár, A. G. *J. Am. Chem. Soc.* **1992**, *114*, 9568.
(84) Jensen, J. H.; Gordon, M. S. *J. Am. Chem. Soc.* **1991**, *113*, 7971.
(85) Zhang, K.; Chung-Phillips, A. *J. Phys. Chem. A* **1998**, *102*, 3625.